Shock and Vibration 12 (2005) 349–361
IOS Press

Improving robustness of tuned vibration absorbers using shape memory alloys

Mohammad H. Elahinia[a], Jeong-Hoi Koo[b] and Honghao Tan[c]
[a]*Dynamic and Smart Systems Laboratory, Mechanical Industrial and Manufacturing Engineering Department, The University of Toledo, 2801 West Bancroft MS312, Toledo, OH 43606, USA*
Tel.: +1 419 530 8224; Fax: +1 419 530 8206; E-mail: mohammad.elahinia@utoledo.edu
[b]*Department of Manufacturing and Mechanical Engineering Miami University, Oxford, OH 45056, USA*
E-mail: koo@muohio.edu
[c]*Dynamic and Smart Systems Laboratory, Mechanical Industrial and Manufacturing Engineering Department, The University of Toledo, USA*
E-mail: htan@utoledo.edu

Received 14 January 2005
Revised 24 January 2005

Abstract. A conventional passive tuned vibration absorber (TVA) is effective when it is precisely tuned to the frequency of a vibration mode; otherwise, it may amplify the vibrations of the primary system. In many applications, the frequency often changes over time. For example, adding or subtracting external mass on the existing primary system results in changes in the system's natural frequency. The frequency changes of the primary system can significantly degrade the performance of TVA. To cope with this problem, many alternative TVAs (such as semiactive, adaptive, and active TVAs) have been studied. As another alternative, this paper investigates the use of Shape Memory Alloys (SMAs) in passive TVAs in order to improve the robustness of the TVAs subject to mass change in the primary system. The proposed SMA-TVA employs SMA wires, which exhibit variable stiffness, as the spring element of the TVA. This allows us to tune effective stiffness of the TVA to adapt to the changes in the primary system's natural frequency. The simulation model, presented in this paper, contains the dynamics of the TVA along with the SMA wire model that includes phase transformation, heat transfer, and the constitutive relations. Additionally, a PID controller is included for regulating the applied voltage to the SMA wires in order to maintain the desired stiffness. The robustness analysis is then performed on both the SMA-TVA and the equivalent passive TVA. For our robustness analysis, the mass of the primary system is varied by $\pm$ 30% of its nominal mass. The simulation results show that the SMA-TVA is more robust than the equivalent passive TVA in reducing peak vibrations in the primary system subject to change of its mass.

Keywords: Shape memory alloy, tuned vibration absorber, modeling, control

1. Introduction

Tuned Vibration Absorbers (TVAs) have been effective engineering devices to suppress vibrations of machines and structures since their invention in the early 1900s. A vibration absorber is a vibratory subsystem attached to a primary system. It normally consists of a mass, a spring and a damper. Mounted on the primary system, a TVA counteracts the motions of primary system, "absorbing" vibrations of the primary structure. However, a conventional passive TVA is only effective when it is tuned properly; otherwise, it can magnify the vibration levels of the primary system -hence, the name "tuned" vibration absorber. In many practical applications, inevitable off-tuning of a TVA often occurs because of inheritance of systems' operation conditions and system parameter changes with time. To cope with these problems, extensive studies have been done towards the advancements of passive TVAs with new designs and concepts for TVAs during the past two decades. Theses designs include adaptive, semi-active, and

ISSN 1070-9622/05/$17.00

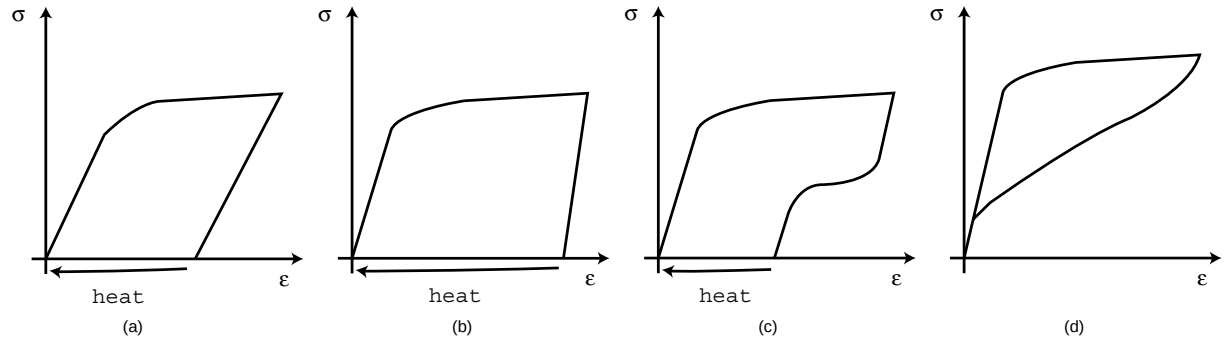

Fig. 1. Mechanical behavior of the shape memory alloy. ξ_0 indicates the initial phase state (martensite fraction) for each case (a) $T < A_s$, $\xi_0 = 1$ (b) $M_s < T < A_s, \xi_0 = 0$ (c) $A_s < T < A_f, \xi_0 = 0$ (d) $T > A_f, \xi_0 = 0$ [3].

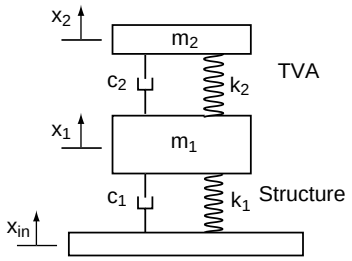

Fig. 2. A base-excited passive TVA model.

active TVAs. A comprehensive review of configurations, developments, and applications of TVAs can be found in the papers by Sun et al. in [16], Housner et al. [5], Symans and Constaninou [17], and Soong and Spencer [15].

SMAs have unique thermomechanical behaviors such as shape memory effect and pseudoelasticity, which have made them attractive candidates for structural vibration control applications [14]. Willimas et al. have studied adaptive vibration absorbers using SMA wires [18]. They experimentally showed that by activating different number of SMA wires various tuned frequencies can be achieved. Khan et al. [6] and Lagoudas et al. [7] used SMA tubes for passive vibration isolation. They showed the robustness of the resulting isolator through both simulations and experiments. More recently, Rustighi et al. [13] designed and experimentally evaluated an SMA- TVA, with an SMA beam element as the extra degree-of-freedom. In their experiment, the SMA-TVA achieved a frequency change of 21.4% due to the variation in the stiffness of the SMA element. In the experiments, which were performed open-loop, the effect of temperature on the frequency of TVA were measured.

As an alternative method to passive TVAs, this study considers an SMA TVA that uses SMA wires, which can provide variable stiffness. To this end, a control system is designed to continuously adjust the applied voltage to the SMA elements in order to maintain the desired temperature and stiffness. The focus of this study will be modeling and the design of control system for SMA TVAs and evaluation of their behavior subjected to mass off-tuning of the primary system. The performance of SMA TVA will be compared with the equivalent passive TVA to analyze the relative benefits. The thermomechanical behavior of the SMA element is presented with a simple phenomenological model that does not include the effect of strain rate. It is expected that using a more comprehensive SMA model for simulations will result in closer match of the simulations with experiments albeit adding complexity to simulations and control systems design. After providing background information of SMA materials, design of TVAs that include modeling of SMA TVA will be presented. The control system design for re-tuning the TVA is described followed by a detailed analysis of simulation results of both passive and SMA TVAs, which will conclude this paper.

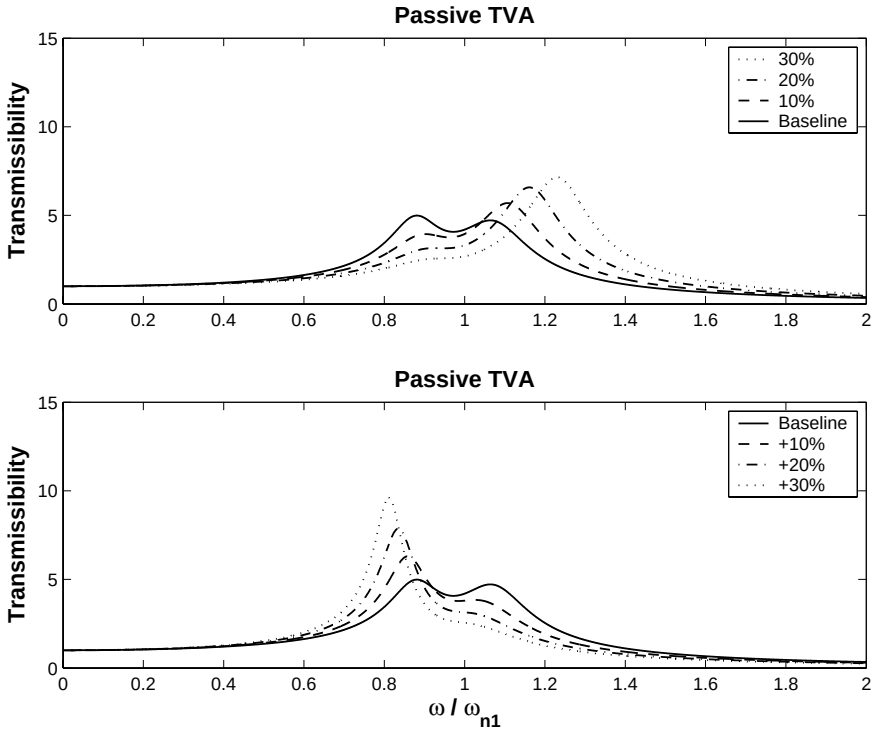

Fig. 3. Peak transmissibility variation of the passive TVA: (a) decreasing the primary mass (b) increasing the primary mass.

2. Background

Shape Memory Alloys are group of metallic alloys that exhibit the characteristics of either large recoverable strains or large force due to temperature and/or load changes. The unique thermomechanical properties of the SMAs are due to the phase transformation from the austenite (parent) phase to martensite (product) phase and vice versa. These transformations take place because of changes in the temperature, or stress, or a combination of both. In a stress-free state, an SMA material at high temperature exists in the parent phase. The parent or austenite phase usually is a body centered cubic crystal structure. When the temperature of the material decreases, the phase transforms into martensite which is usually a face centered cubic structure. In the stress-free state, the martensite is in twinned martensite state, that is, it exist in multiple variants that are crystallographically similar but are oriented in different habit planes. Upon loading, still in martensite phase, the material changes to a single variant phase.

We can separate the mechanical behavior of SMAs into two categories: the shape memory effect and pseudoelastic effect. In shape memory effect, SMAs exhibit a large residual strain after undergoing loading and unloading. This strain can be fully recovered upon heating the material. In pseudoelastic effect the SMA materials provide a large stain upon loading that is fully recoverable in a hysteresis loop upon unloading [3,10]. These effects are illustrated in Fig. 1.

3. Design of tuned vibration absorbers

In this section, the tuning and design process of the tuned vibration absorbers are explained. The passive TVAs and their limitations are discussed in Section 3.1. The passive TVAs become off-tuned and their performance degrades if the parameters of the system, namely the primary mass and/or stiffness, change. To overcome the off-tuning problem of the passive TVA we have used SMA wires to design an active TVA. The design process of the SMA TVA is explained in Sections 3.2 and 3.3.

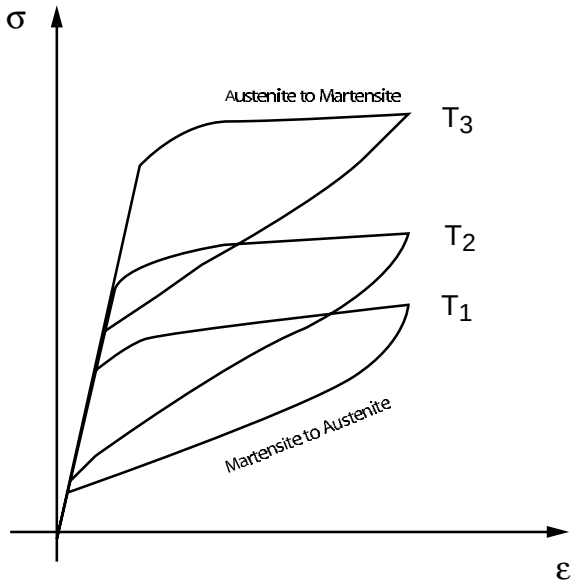

Fig. 4. Isothermal mechanical behavior of the shape memory alloy, $A_s < T_1 < T_2 < T_3$.

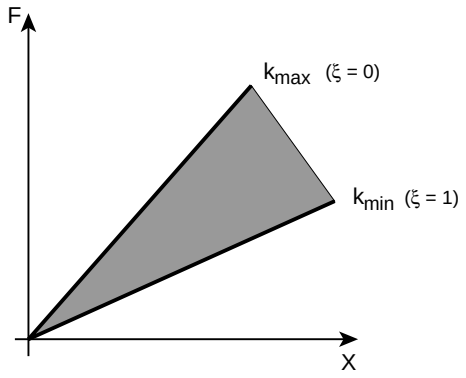

Fig. 5. The stiffness of the SMA wire changes as a result of phase transformation.

3.1. Passive tuned vibration absorbers

A two-degree of freedom passive TVA model is presented in Fig. 2. The mass of the primary structure and the absorber are defined by m_1 and m_2, with their corresponding displacements defined by x_1 and x_2. The absorber spring, k_2, and damper, c_2, are mounted on the primary mass. The stiffness and damping of the primary structure are represented by k_1 and c_1, respectively. The transmissibility equation for this system can be written as:

$$\frac{X_1}{X_{\text{in}}} = \frac{m_2 s^2 + c_2 s + k_2}{(m_1 s^2 + (c_1 + c_2)s + k_1 + k_2)(m_2 s^2 + c_2 s + k_2) - (c_2 s + k_2)^2} \tag{1}$$

Equation (1) can be rewritten in a non-dimensional form $\frac{X_1}{X_{\text{in}}} = \frac{A(s)}{B(s)}$, where

$$\begin{aligned} A(r) &= (1 + 2\zeta_1 rj)(g^2 - r^2 + 2\zeta_2 grj) \\ B(r) &= (-r^2 + 2rj(\zeta_1 + \zeta_2 g\mu) + 1 + \mu g^2)(-r^2 + 2\zeta_2 rgj + g^2 - \mu(2\zeta_2 grj + g^2))^2 \end{aligned} \tag{2}$$

The parameters used in Eq. (2) are defines as:

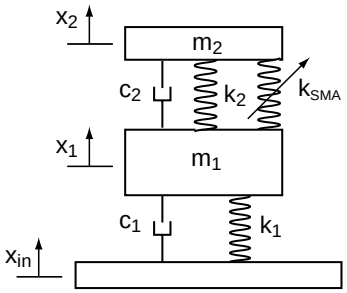

Fig. 6. A tuned vibration absorber model with variable stiffness SMA wires.

$\omega_{n1} = \sqrt{\frac{k_1}{m_1}}$ natural frequency of primary structure,

$\omega_{n2} = \sqrt{\frac{k_2}{m_2}}$ natural frequency of TVA,

$\zeta_1 = \frac{c_1}{2\omega_{n1}m_1}$ damping ratio of primary structure,

$\zeta_2 = \frac{c_2}{2\omega_{n2}m_2}$ damping ratio of TVA,

$\mu = \frac{m_2}{m_1}$ mass ratio (TVA mass/structure mass),

$g = \frac{\omega_{n2}}{\omega_{n1}}$ natural frequency ratio (TVA/structure), and

$r = \frac{\omega}{\omega_{n1}}$ forcing frequency ratio.

Assuming that the damping of the primary mass is negligible (i.e., $\zeta_1 = 0$), the optimum tuning condition can be written as follows [12].

$$\begin{aligned} k_2 &= m_2 \left(\frac{w_{n1}}{(1+\mu)} \right)^2 \\ \zeta_2 &= \sqrt{\frac{3\mu}{8(1+\mu)^3}} \end{aligned} \tag{3}$$

3.2. SMA tuned vibration absorbers

When the parameters of the main system change, the tuning condition, shown in Eq. (3), will no longer be optimal and as a result, the TVA will be less effective. Figure 3 shows how the transmissibility of a passive TVA changes as the TVA off-tunes. The off-tuning in these simulations is caused by variation in the primary mass. The performance of the passive TVA is worse for both increased as well as decreased values of the primary mass.

In this section, the idea of using SMA wires to adjust the stiffness of the TVA, as a way to re-tune the TVA, is explained. A design procedure, showing the effective range of variation of the SMA stiffness and a procedure for selecting the appropriate SMA wire is also presented.

The quasistatic mechanical behavior of the shape memory alloys, at constant temperature, is shown in Fig. 4. The effective stiffness of an SMA wire, when the temperature is constant and there is no phase transformation, can be written as [8]:

$$\begin{aligned} \sigma &= E(\xi)\varepsilon \\ E(\xi) &= E_A + \xi(E_M - E_A) \\ k_{SMA} &= F/\Delta x = E(\xi)A/l_0 \end{aligned} \tag{4}$$

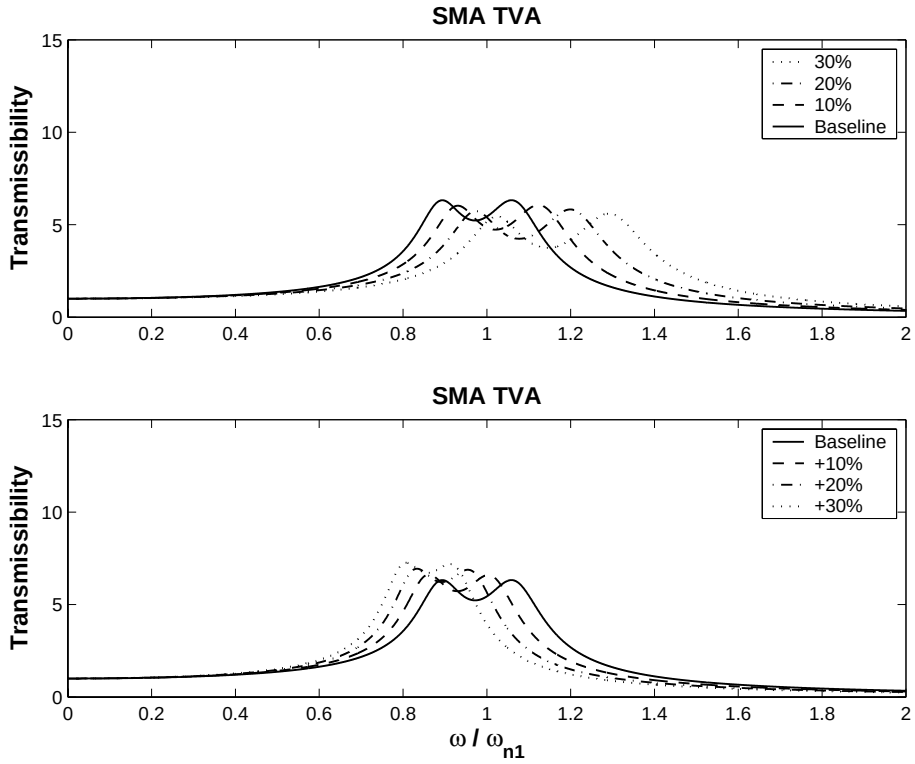

Fig. 7. Peak transmissibility variation of the SMA TVA: (a) decreasing the primary mass (b) increasing the primary mass.

where σ, ε, l_0, A, and Δx are the stress, strain, initial length, cross section area, and deflection of the SMA wire, respectively. Also, E is the Young's modulus and subscripts A and M indicate the austenite and martensite phases respectively; where $E_A > E_M$. This way, the stiffness of the wire is a function ξ; this stiffness, as illustrated in Fig. 5, is maximum when the wire is in the austenite phase ($\xi = 0$ and $E = E_A$). Likewise, the minimum stiffness is obtained when the wire is in the martensite phase ($\xi = 1$ and $E = E_M$). When $0 < \xi < 1$, the instantaneous stiffness of the SMA wire is between the two extreme values.

The behavior of SMA described by the phenomenological models of Liang [8] and Brinson [3] do not include the effect of fast strain rates nor they cover the effect of cyclic loadings. These models, as presented in Section 4.2, are merely chosen for the simplicity. The control system designed in this work regulates the applied voltage to the SMA wires in order to maintain the instantaneous stiffness of the SMA wires at the desired stiffness based on the above mentioned models. The control system can, however, be altered based on more complex models that include the strain rate and cyclic loading effects.

When SMA wires are used in parallel to regular springs as variable stiffness elements, as shown in Fig. 6, the stiffness can be adjusted by changing phase of the SMA wires. The percentage change in the stiffness depends only on the Young's modulus of the two phases of the SMA material and does not depend on the geometry of the SMA element as shown below.

$$\frac{k_{\max} - k_{\min}}{k_{\min}} = k_{\mathrm{SMA-range}} = \frac{E_A - E_M}{E_M} \tag{5}$$

As an example, if Flexinol wire is used the possible percentage increase in the stiffness is 167.9% ($E_A = 75$ GPa and $E_M = 28$ GPa).

Figure 7 illustrates the transmissibility of the SMA TVA. In the simulations, assuming that the required stiffness can be achieved instantaneously, the primary mass is changed by $\pm$ 30%. The stiffness of SMA wires is adjusted such that the tuning condition, presented in Eq. (3), is satisfied. As a result, the peak transmissibility remains similar for systems with different primary masses.

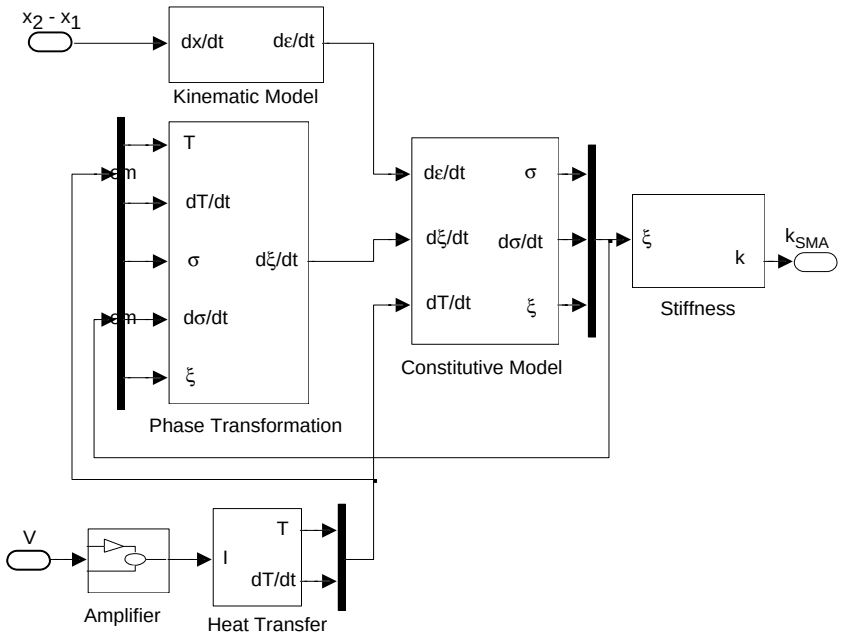

Fig. 8. Block diagram showing the SMA wire's model.

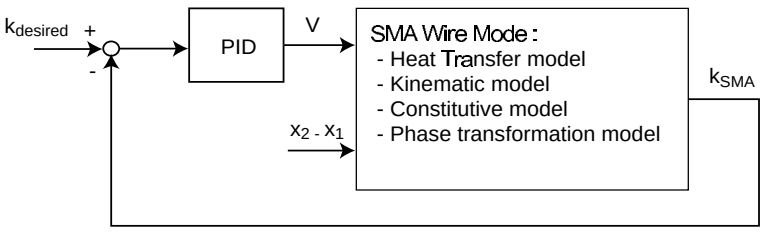

Fig. 9. Stiffness control for the tuned vibration absorber with SMA wires for variable stiffness.

3.3. Design parameters

The cross section area, the un-deformed length of the SMA wire, and the number of wires are the three design parameters of the SMA TVA. The initial length of the SMA wires is defined based on the maximum relative displacement of the absorber and the primary masses. For example if the maximum net displacement between the absorber and primary masses is limited to 10 cm, a 1 m long SMA wire, undergoing a 10% strain, can accommodate this displacement.

Based on the required tuning frequency variation we can calculate the required stiffness range, i.e. k_{High} and k_{Low}. Using the stiffness change provided by the SMA wires (Eq. (5)), one can calculate the three unknowns of the following equations, i.e. the stiffness of regular spring (k_2), the required maximum ($k_{\max}$), and the minimum stiffness ($k_{\min}$) of the SMA wires.

$$\begin{aligned} \frac{k_{\max} - k_{\min}}{k_{\min}} &= k_{\mathrm{SMA-range}} \\ k_2 + k_{\max} &= k_{\mathrm{High}} \\ k_2 + k_{\min} &= k_{\mathrm{Low}} \end{aligned} \tag{6}$$

The diameter of the SMA wire can be calculated using Eq. (4).

Table 1
Parameters of the SMA TVA

Parameter	Value (unit)
m_1	1360 (kg)
m_2	68 (kg)
ω_{n1}	4 (Hz)
ζ_1	0.03
E_A	75 (GPa)
E_M	28 (GPa)

$$d = \sqrt{\frac{4l_0k_{\max}}{E_A\pi}} = \sqrt{\frac{4l_0k_{\min}}{E_M\pi}} \tag{7}$$

If the calculated diameter for the wire is larger than that of the available SMA wire, multiple wires can be used.

As an example, let's consider an SMA TVA for which $l_0 = 2$ m, $k_{\text{High}} = 53.4$ kN/m, $k_{\text{Low}} = 30.6$ kN/m, and $k_{\text{SMA}-\text{range}} = 1.679$. Using the design methodology we can calculate:

$$k_2 = 1.705e4\text{N/m}$$
$$k_{\max} = 3.64e^4\text{N/m}$$
$$k_{\min} = 1.36e^4\text{N/m}$$
$$d = \sqrt{\frac{4 \times 2 \times 1.36e^4}{28e^9 \times \pi}} = 0.0011\text{m}$$

With 150 μ m-diameter SMA wires, 8 wires are needed in order to provide the required tuning range.

4. Modeling of SMA TVAs

In this section, the model of the SMA wire used for the simulation is presented. The SMA wire's model, as illustrated in Fig. 8, consists of three parts: (1) the kinematic model, (2) the SMA thermomechanical model, and (3) the heat transfer model. The SMA wire is a Flexinol wire with the diameter of 150 μ m. Heating the SMA wire, while the stress is kept constant, induces a phase transformation and negative strain in the material. Conversely, cooling the wire induces positive strain. The following sections present, in detail, the system model used in subsequent simulations.

4.1. Kinematic model

The strain of the wire is caused by the relative motion of the primary and absorber masses. Therefore, the SMA wire strain rate $\dot{\varepsilon}$ and relative velocity of the two masses $\dot{x}$ are related kinematically as:

$$\dot{\varepsilon} = \frac{\dot{x}}{l_0} \tag{8}$$

where $x = x_2 - x_1$ is the relative displacement of the two masses and l_0 is the initial length of the SMA wire.

4.2. Thermomechanical model

Based on the works of Liang and Rogers [8,9] and Brinson [3], the thermomechanical behavior of SMAs can be described in terms of strain (ϵ), martensite fraction (ξ), and temperature (T). In the most general form, the thermomechanical constitutive equation is

$$d\sigma = D(\epsilon, \xi, T)d\epsilon + \Omega(\epsilon, \xi, T)d\xi + \Theta(\epsilon, \xi, T)dT \tag{9}$$

where $D(\epsilon, \xi, T)$ is representative of the modulus of the SMA material, $\Omega(\epsilon, \xi, T)$ is the transformational tensor, and $\Theta(\epsilon, \xi, T)$ is related to the thermal coefficient of expansion.

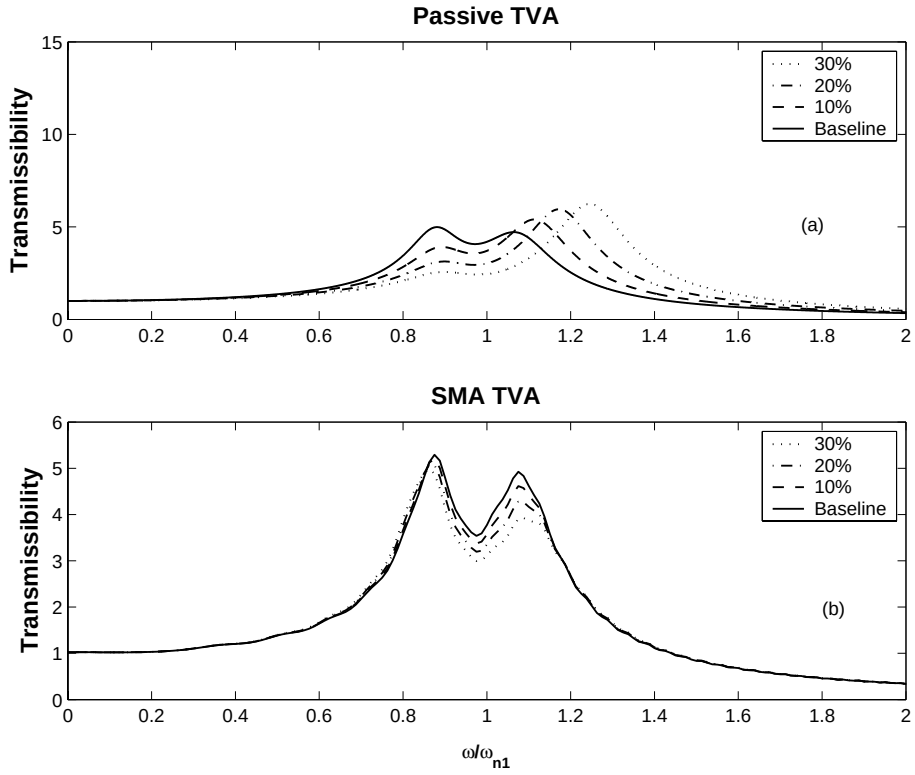

Fig. 10. Peak transmissibility variation, reducing the primary mass by 30%: (a) passive TVA (b) SMA TVA.

The shape memory effect is caused by the phase transformation of the molecular structure between martensite and austenite. The transformation from austenite to martensite is described by:

$$\xi = \frac{1-\xi_0}{2}\cos\left[a_M\left(T - M_f - \frac{\sigma}{C_M}\right)\right] + \frac{1+\xi_0}{2} \tag{10}$$

for $C_M(T - M_s) < \sigma < C_M(T - M_f)$ and the transformation from martensite to austenite is described by:

$$\xi = \frac{\xi_0}{2}\cos\left[a_A\left(T - A_s - \frac{\sigma}{C_A}\right)\right] + 1 \tag{11}$$

for $C_A(T - A_f) < \sigma < C_A(T - A_s)$, where ξ_0 is the martensite fraction prior to the current transformation, M_s and M_f are the martensite phase start and final temperatures, A_s and A_f are the austenite phase start and final temperatures, and a_M and a_A are defined by:

$$a_M = \frac{\pi}{M_s - M_f}, \quad a_A = \frac{\pi}{A_f - A_s} \tag{12}$$

The constants C_A and C_M are material properties that describe the relationship–assumed to be linear–between temperature and the critical stress to induce transformation.

4.3. Heat transfer model

The heat transfer model of the wire, using the principle of conservation of energy, is written as:

$$mC_p\frac{dT}{dt} = I^2R(\xi) - h(T)A(T - T_\infty) - m\Delta H\dot{\xi} \tag{13}$$

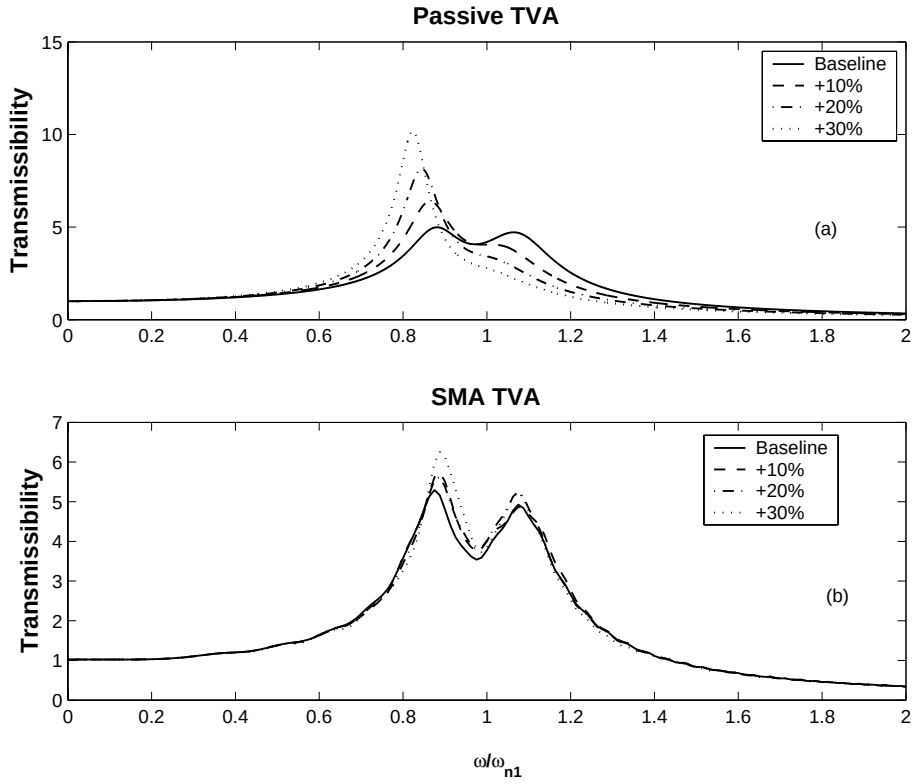

Fig. 11. Peak transmissibility variation, increasing the primary mass by 30%: (a) passive TVA (b) SMA TVA.

where C_p is the specific heat, I and R are electric current and resistance respectively, $h(T)$ is the convection heat transfer, A is the circumference area of the wire, T and T_∞ are the temperature of the wire and ambient, respectively, ΔH is the latent heat associated with the phase transformation [11]. This equation presents the effect of the Joule heating, convection heat transfer, and latent heat on the internal energy of the wire. More details of the heat transfer analysis can be found in Appendix A.

4.4. Controller design

The model also includes a PID controller. The PID controller is to minimize the error of the absorber stiffness by regulating the voltage to the SMA wire. The schematic of the control algorithm for the SMA TVA is shown in Fig. 9. It is assumed that the primary mass is the only variable parameter and its value is known. Therefore, the desired change in stiffness of the TVA is known. It is also assumed that the relative displacement of the primary and TVA masses is measured. As the block-diagram of the SMA TVA control system illustrates in Fig. 9, the stiffness of the wire is calculated using Eq. (4) as:

$$k_{\mathrm{SMA}} = \frac{n^2 E(\xi) A}{l_0} \tag{14}$$

where n is the number of SMA wires.

5. Results

In this section the results of off-tuning simulations are presented. In the simulations, the three-part model of the SMA wire is used along with the PID controller. For the off-tuning analysis, the primary mass is varied by $\pm$ 30%

Table 2
Air properties as a function of the SMA wire temperature, the ambient temperature assumed to be $T_\infty = 23^\circ\mathrm{C}$

$T_w^\circ\mathrm{C}$	$T_f(\mathrm{K})$	$k(\mathrm{W/m^\circ C})$	$\alpha(\mathrm{m^2/s})$	$\nu(\mathrm{m^2/s})$	Pr
31	300	0.0261	2.21e-5	1.57e-5	0.712
51	310	0.0268	2.35e-5	1.67e-5	0.711
71	320	0.0275	2.49e-5	1.77e-5	0.710
91	330	0.0283	2.64e-5	1.86e-5	0.708
111	340	0.0290	2.78e-5	1.96e-5	0.707

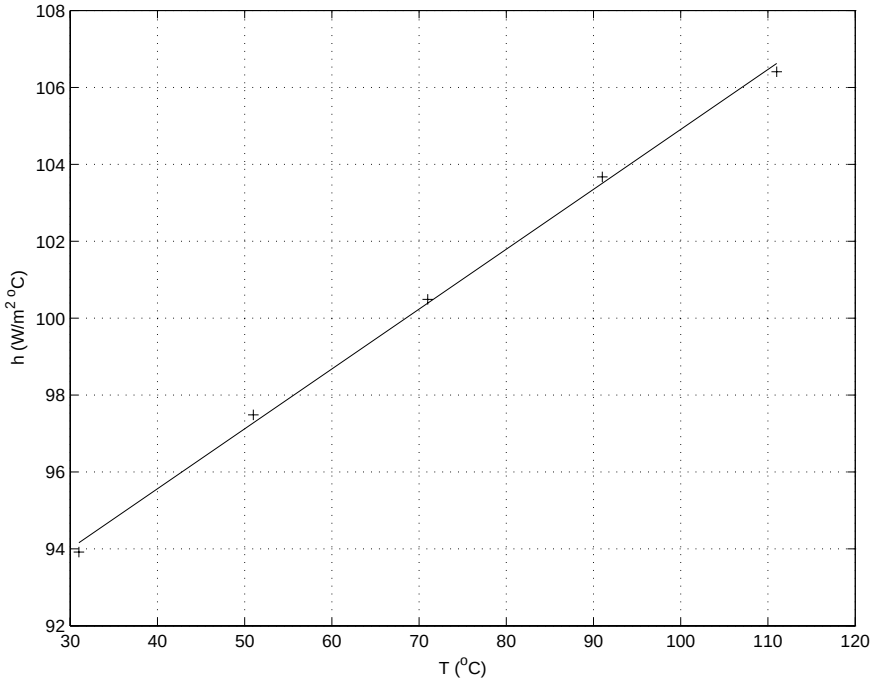

Fig. 12. The convection heat transfer coefficient as the function of the SMA wire temperature.

of its original value. For each case, the desired stiffness is calculated using Eq. (3); in the simulation, this stiffness is then compared with the stiffness of the SMA wires, calculated from Eq. (14), the PID controller adjusts the voltage to the SMA wires in order to maintain the desired stiffness. The simulations are performed using a chirp displacement input. The amplitude of the input signal is 0.01 m, and the frequency range is between 0.1 Hz and 20 Hz. The parameters of the TVA system are shown in Table 1.

Figure 10 compares the transmissibility of the passive and SMA TVAs, when the primary mass is reduced by 30%. For the passive TVA, shown in Fig. 10(a), decreasing the primary mass significantly increases the peak transmissibility. On the other hand, for the SMA TVA, shown in Fig. 10(b), the peak transmissibility does not increase. In fact the peak transmissibility decreases as the primary mass decreases. The transmissibility for the passive and SMA TVAs, for increasing primary mass, is presented in Fig. 11. The peak transmissibility for the SMA TVA, shown in Fig. 11(b), increases, but still the peaks remain lower than the peaks for the passive TVA, shown in Fig. 11(a). This indicates that the SMA TVA outperforms the passive TVA in reducing the maximum vibration level.

6. Conclusions

This paper investigated an SMA TVA as a new alternative method to improve conventional passive TVAs. The SMA TVA considered in this paper is an augmented TVA that uses SMA wires as the variable stiffness element. As

such, the SMA TVA has an ability to change its frequency by adjusting its stiffness. After providing detailed design procedures, we developed a model for the SMA TVA. The model includes the thermomechanical behavior, phase transformation, and heat transfer model of the SMA wire. Using this TVA model, we performed mass off-tuning tests to evaluate dynamic performance of the SMA TVA, along with the equivalent passive TVA. For the off-tuning tests, the primary system's mass was varied $\pm$ 30% of its original mass. To control the SMA TVA, we used a PID controller that determined and provided control voltage to the SMA wires. The simulation results showed that SMA TVA is more robust to changes in the primary system's mass. Moreover, the results showed that SMA TVA outperformed the equivalent passive TVA in reducing maximum vibrations of the primary system.

References

[1] A. Bhattacharyya, D.C.A. Lagoudas, Y. Wang and V.K. Kinra, On the role of thermoelectric heat transfer in the design of sma actuators: theoretical modeling and experiments, *Smart materials and structures* **4** (1995), 252–263.

[2] A. Bhattacharyya, L. Sweeney and M.G. Faulkner, Experimental characterization of free convection during thermal phase transformation in shape memory alloy wires, *Smart materials and structures* **11** (2002), 411–422.

[3] L.C. Brinson, One-dimensional constitutive behavior of shape memory alloys: Thermomechanical derivation with non-constant material functions and redefined martensite internal variable, *Journal of intelligent material systems and structures* **4** (April, 1993), 229–242.

[4] Y.A. Çengel, *Heat Transfer A Practical Approach*, McGraw-Hill, Inc., Princeton Road, S-1 Nightstown, NJ 08520, second edition, 1998.

[5] L.A. Housner, G.W. Bergman, A.G. Claus, R.O. Caughey, T.K. Chassiakos, S.F. Masri, S.E. Skelton, T.T. Soong, B.F. Spencer and J.T.P. Yao, Structural control: Past, present, and future, *Journal of Engineering Mechanics* **123**(9) (1997), 897–971.

[6] M.M. Khan, D.C. Lagoudas, J.J. Mayer and B.K. Henderson, Pseudoelastic SMA Spring Elements for Passive Vibration Isolation: Part I – Modeling, *Journal of Intelligent Material Systems and Structures* **15**(6) (June, 2004), 413–442.

[7] D.C. Lagoudas, M.M. Khan, J.J. Mayer and B.K. Henderson, Pseudoelastic SMA Spring Elements for Passive Vibration Isolation: Part II – Simulation and Experimental Correlations, *Journal of Intelligent Material Systems and Structures* **15**(6) (June, 2004), 413–442.

[8] C. Liang and C.A. Rogers, One-dimensional thermomechanical constitutive relations for shape memory materials, *Journal of Intelligent Material Systems and Structures* **1**(2) (1990), 207–234.

[9] C. Liang and C.A. Rogers, Design of shape memory alloy actuators, *Journal of Mechanical Design* **114** (1993), 23–30.

[10] Y. Matsuzaki and H. Naito, Macroscopic and microscopic constitutive models for shape memory alloys based on phase interaction energy unction: a review, *Journal of Intelligent Material Systems and Structures* **15** (February, 2004), 141–155.

[11] P.L. Potapov and E.P. da Silva, Time response of shape memory alloy actuators, *Journal of intelligent material systems and structures* **11** (February 2000), 125–134.

[12] S.S. Rao, *Mechanical Vibrations*, Addison-Wesley Publishing Company, third edition, 1995.

[13] E. Rustighi, M.J. Brennan and B.R. Mace, A shape memory alloy adaptive tuned vibration absorber: design and implementation, *Smart Materials and Structures* **14**(2) (February, 2005), 19–28.

[14] S. Saadat, J. Salichs, M. Noori, Z. Hou, H. Davoodi, I. Bar-On, Y. Suzuki and A. Masuda, An overview of vibration and seismic applications of niti shape memory alloy, *Smart Materials and Structures* **11** (2002), 218–229.

[15] T.T. Soong and B.F.Jr. Spencer, Supplemental energy dissipation: state-of-the-art and state-of-the-practice, *Journal of Engineering Structures* **24** (2002), 243–259.

[16] J.Q. Sun, M.R. Jolly and M.A. Norris, Passive, adaptive and active tuned vibration absorbers- a survey, *Transactions of the ASME, 50th Anniversary of the Design Engineering Division* **117** (1995), 234–242.

[17] M.D. Symans and M.C. Constantinou, Semi-active control systems for seismic protection of structures: A state-of-art review, *Journal of Engineering Structures* **21** (1999), 469–487.

[18] K. Williams, G. Chiu and R. Bernhard, Adaptive-passive absorbers using shape-memory alloys, *Journal of Sound and Vibration* **249**(5) (2002), 835–848.

Appendix A: SMA heat transfer analysis

There are number of studies on the heat transfer of the SMA materials. A representative example is the work of Bhattacharyya et al. [1] in which the possibility of using thermoelectric effect in order to improve the cooling response of the SMA actuators was studied. Bhattacharyya et al. [2] also worked on the characterization of the convection heat transfer coefficient for SMA wires. They modeled the coefficient as a linear function of the current applied to the wire and performed experiments with SMA and non-SMA wires to verify the model. Potapov and da Silva [11] used Liang's kinematics model for SMA elements with constant stress and constant strain in order to find both heating and cooling response times. They assumed the convection heat transfer to be constant and showed the time constant is in agreement with the experiments.

Here we have used the principle of the conservation of energy to model the heat transfer behavior of the SMA wire. Unlike the works of Bhattacharyya et al. [2] and Potapov and da Silva [11] we have used a convection heat transfer coefficient that is based on the thin cylinder theory. As explained next the convection coefficient is found to be a function of the wire temperature.

The heat transfer model of the wire, using the principle of conservation of energy, is written as

$$mC_p \frac{dT}{dt} = I^2 R(\xi) - h(T)A(T - T_\infty) - m\Delta H\dot{\xi} \tag{15}$$

where C_p is the specific heat, I and R are electric current and resistance respectively, $h(T)$ is the convection heat transfer, A is the circumference area of the wire, T and T_∞ are the temperature of the wire and ambient, respectively, ΔH is the latent heat associated with the phase transformation [11]. This equation presents the effect of the Joule heating, convection heat transfer, and latent heat on the internal energy of the wire.

Natural heat convection takes place because of Buouyoncy force and the difference between cold and warm air densities. Because of the temperature difference between the vertical surfaces, in this case a cylindrical surface, and the ambient a boundary layer flow develops over the lateral surface. When the boundary layer thickness is smaller than the cylinder diameter, the cylinder can be modeled as a vertical wall ignoring its curvature. In the case of a thin wire, however, the diameter is not necessarily larger than the boundary layer thickness and hence a different Nusselt number and therefore a different convection coefficient should be used. The criteria for considering a cylinder as a vertical wall is:

$$\frac{D}{l} > Ra_l^{-\frac{1}{4}} \tag{16}$$

where D and l are the cylinder's diameter and length, respectively, and Ra_L is the Rayleigh number. It can be shown that for the SMA wire this condition is not satisfied for the range of temperature of interest. On the other hand, for the vertical thin cylinders the Nusselt number is written as:

$$Nu_l = \frac{4}{3}\left[\frac{7Ra_l Pr}{5(20+21Pr)}\right]^{\frac{1}{4}} + \frac{4(272+315Pr)l}{35(64+63Pr)D} \tag{17}$$

where Pr is the Prandtl number, $Nu_l = hl/k$, and $Ra_l = g\beta\Delta T l^3/\alpha\nu$. In these definitions h is the length-averaged heat transfer coefficient, ΔT is the temperature difference between the surface of the ambient. Also β is the volume expansion coefficient that for the ideal gas can be shown to be $\beta = \frac{1}{T}$ where T is the absolute temperature. k, α and ν are thermal conductivity, thermal diffusivity, and kinematic viscosity of the air calculated at the film temperature $T_f = \frac{T+T_\infty}{2}$.

Therefore the convection coefficient is a function of both temperatures of wire and the ambient temperature. We assume that the ambient temperature is constant while the wire's temperatures changes considerably. Table 2 shows the property of the air over the actuation temperature range [4]. The ambient temperature is assumed to be 23 °C. Using these properties the convection coefficient can be calculated. Figure 12 shows the calculated convection heat transfer coefficient which increases as a function of the temperature of the wire. As shown in the figure, we have approximated it with a linear function as $h(T) = 0.1558T + 89.33$, where T is the temperature of the wire in Centigrade.

It is worth noting that the cooling rate is proportional to the ratio of the surface area to the heat capacity. Thus the ratio of the surface area to the volume of the wire is an indicator of the cooling rate. The generating force on the other hand is proportional to the cross sectional area of the wire. The surface area/volume is in inverse proportion to the diameter. Therefore, if the diameter is small, the cooling rate is fast. However, the generating force is much smaller.

Jeong-Hoi Koo
Assistant Professor
Department of Manufacturing and Mechanical Engineering
Miami University
Oxford, OH 45056
E-mail: koo@muohio.edu